

# Human Anti-A $\beta$ IgGs Target Conformational Epitopes on Synthetic Dimer Assemblies and the AD Brain-Derived Peptide

Alfred T. Welzel<sup>1</sup>, Angela D. Williams<sup>2</sup>, Helen P. McWilliams-Koeppen<sup>2</sup>, Luis Acero<sup>2</sup>, Alfred Weber<sup>3</sup>, Veronika Blinder<sup>4</sup>, Alex Mably<sup>1,4</sup>, Sebastian Bunk<sup>3</sup>, Corinna Hermann<sup>3</sup>, Michael A. Farrell<sup>5</sup>, Hartmut J. Ehrlich<sup>3</sup>, Hans P. Schwarz<sup>3</sup>, Dominic M. Walsh<sup>1,4</sup>, Alan Solomon<sup>2</sup>, Brian O'Nuallain<sup>1,2,4\*</sup>

**1** The Conway Institute, University College Dublin, Belfield, Dublin, Republic of Ireland, **2** Human Immunology and Cancer Program, Department of Medicine, University of Tennessee Graduate School of Medicine, Knoxville, Tennessee, United States of America, **3** Baxter BioScience, Vienna, Austria, **4** The Laboratory of Neurodegenerative Research, Brigham and Women's Hospital, Harvard Institutes of Medicine, Boston, Massachusetts, United States of America, **5** Dublin Brain Bank, Pathology Department, Beaumont Hospital, Dublin, Ireland

## Abstract

Soluble non-fibrillar assemblies of amyloid-beta (A $\beta$ ) and aggregated tau protein are the proximate synaptotoxic species associated with Alzheimer's disease (AD). Anti-A $\beta$  immunotherapy is a promising and advanced therapeutic strategy, but the precise A $\beta$  species to target is not yet known. Previously, we and others have shown that natural human IgGs (NABs) target diverse A $\beta$  conformers and have therapeutic potential. We now demonstrate that these antibodies bound with nM avidity to conformational epitopes on plate-immobilized synthetic A $\beta$  dimer assemblies, including synaptotoxic protofibrils, and targeted these conformers in solution. Importantly, NABs also recognized A $\beta$  extracted from the water-soluble phase of human AD brain, including species that migrated on denaturing PAGE as SDS-stable dimers. The critical reliance on A $\beta$ 's conformational state for NAB binding, and not a linear sequence epitope, was confirmed by the antibody's nM reactivity with plate-immobilized protofibrils, and weak  $\mu$ M binding to synthetic A $\beta$  monomers and peptide fragments. The antibody's lack of reactivity against a linear sequence epitope was confirmed by our ability to isolate anti-A $\beta$  NABs from intravenous immunoglobulin using affinity matrices, immunoglobulin light chain fibrils and Cibacron blue, which had no sequence similarity with the peptide. These findings suggest that further investigations on the molecular basis and the therapeutic/diagnostic potential of anti-A $\beta$  NABs are warranted.

**Citation:** Welzel AT, Williams AD, McWilliams-Koeppen HP, Acero L, Weber A, et al. (2012) Human Anti-A $\beta$  IgGs Target Conformational Epitopes on Synthetic Dimer Assemblies and the AD Brain-Derived Peptide. PLoS ONE 7(11): e50317. doi:10.1371/journal.pone.0050317

**Editor:** Yanmin Yang, Stanford University School of Medicine, United States of America

**Received:** July 20, 2012; **Accepted:** October 18, 2012; **Published:** November 27, 2012

**Copyright:** © 2012 Welzel et al. This is an open-access article distributed under the terms of the Creative Commons Attribution License, which permits unrestricted use, distribution, and reproduction in any medium, provided the original author and source are credited.

**Funding:** This work was supported in part by funding from Baxter AG (BO and AS), and the European Community 7th Framework Programme (FP7/2007–2013) under grant agreement No. 200611 (DMW). The funders had no role in study design, data collection and analysis, decision to publish, or preparation of the manuscript.

**Competing Interests:** This work was supported in part by funding from Baxter BioScience, the employer of AW, HJE and HPS, and the European Community 7th Framework Programme (FP7/2007–2013) under grant agreement No. 200611 (DMW). Intravenous immunoglobulin (IVIg; Gammagard liquid®) was provided by Baxter BioScience (Vienna, Austria), and is a Baxter Bioscience product. BO has served as a member of a Baxter preclinical Scientific Advisory Board. DMW is a consultant, shareholder and member of the scientific advisory board of Senexis plc. There are no further patents, products in development or marketed products to declare. This does not alter the authors' adherence to all the PLOS ONE policies on sharing data and materials.

\* E-mail: bonuallain@partners.org

## Introduction

Alzheimer's disease (AD) is a devastatingly common age-related disorder that progressively affects regions of the brain that are associated with higher cognitive functions, such as memory and learning [1]. Pathological hallmarks of AD include, extracellular neuritic deposits of fibrillar A $\beta$ , a 38–43 peptide fragment of the amyloid precursor protein, intraneuronal neurofibrillary tangles of hyperphosphorylated tau protein, synaptic loss and cortical atrophy [2]. Increasing experimental evidence indicates that soluble A $\beta$  aggregates are an upstream pathological species that may cause neuronal compromise through a variety of different not mutually exclusive mechanisms, including toxicity that is associated with prion protein, and which occurs in synergy with hyperphosphorylated tau [3,4].

Although current therapy for AD is only palliative, extensive *in vitro* and *in vivo* studies indicate that anti-A $\beta$  immunotherapy may potentiate the disease for some patients [2,5,6]. However, results have been mixed for recent clinical trials that focused on passive or active vaccination of anti-A $\beta$  antibodies for AD [5,6]. Presumably this is because the disease was treated at an advanced stage and/or it is not clear if these antibodies targeted the most pathogenic A $\beta$  species. Nevertheless, anti-A $\beta$  therapy remains one of the most promising approaches for AD, and a reagent that slows disease progression by about a decade may be sufficient to reduce its incidence by a third [7]. To-date, most passive immunotherapy trials have used humanized anti-A $\beta$  monoclonal antibodies that recognize linear sequence epitopes, and react with multiple A $\beta$  conformers, including native non-pathogenic monomers. An alternative therapeutic approach is to supplement a patient's naturally occurring antibody (NAb) response against pathogenic

A $\beta$  since these antibodies may decrease with aging and AD [8,9]. To-date, four open-label clinical trials, phase's I-II, have been completed on mild to moderate AD patients treated with intravenous immunoglobulin (IVIg; commercially available preparations that consist of a broad spectrum of polyclonal human IgGs purified from 1000's of normal individuals, including anti-A $\beta$  NAbs [10,11]) [12,13]. Although these studies involved small patient numbers and lacked control groups, the results indicate that IVIg was well tolerated, and benefitted some patients by slowing memory decline [12,13]. Given these promising results, two randomized, placebo-controlled phase III and a phase II studies on IVIg for AD are ongoing [12].

Anti-A $\beta$  NAbs mechanism of action on AD is not yet known, and it is possible that in addition to anti-A $\beta$  NAbs, other antibodies, such as anti-inflammatory and immune modulatory IgGs, may act in synergy to benefit an AD patient [14,15]. Nevertheless, results from recent clinical trials have demonstrated IVIg's ability to reduce an AD patient's soluble pool of cerebral A $\beta$  and increase the amount of A $\beta$  in the blood [12,13] – a process consistent with the beneficial effect of anti-A $\beta$  immunotherapy [5,12,13]. Extensive *in vitro* and transgenic mice studies have indicated that anti-A $\beta$  NAbs have therapeutic potential for AD and have multiple mechanisms of action [11,12,16,17,18,19,20], including an ability to neutralize toxic A $\beta$  species [8,18,21]. These antibodies can specifically react with a plethora of synthetic A $\beta$  conformers [11,17,18,19], and cross-react with non-A $\beta$  amyloidogenic aggregates [17,22]. However, it is unclear what portion of their A $\beta$  reactivity is against synaptotoxic A $\beta$  assemblies, and if NAbs have a preference for conformational [23] or linear sequence [24] epitopes. An antibody that recognizes a conformational epitope on synaptotoxic A $\beta$  conformers would have clear therapeutic advantage to an antibody that indiscriminately recognizes a linear sequence epitope on all A $\beta$  species, including physiologically relevant monomeric peptide. Although the precise A $\beta$  species to target is not yet known, substantial experimental evidence suggests that soluble non-fibrillar A $\beta$  aggregates are the proximate synaptotoxic species [25,26,27,28]. Given our current poor understanding on how anti-A $\beta$  NAbs function, we are focused on deciphering NAb's specificity for pathogenically relevant A $\beta$  conformers, and how these interactions may modulate A $\beta$ 's synaptotoxicity. Here we now report investigations on NAb's specificity for conformational and linear sequence A $\beta$  epitopes, synthetic A $\beta$  dimer assemblies, and AD brain-derived A $\beta$ . Our findings strongly indicate that further investigations on the diagnostic/therapeutic relevance of NAb-A $\beta$  interactions are warranted.

## Materials and Methods

### Ethics Statement

Human brain tissue was obtained from the Dublin Brain Bank ([www.brainbank.ie](http://www.brainbank.ie)). The brain bank has written informed consent from patients for all tissue samples, and the collection and processing of brain tissue was approved by the Royal College of Surgeon's in Ireland (RCSI) Ethics Committee. The human brain tissue samples were received and used in accordance with University College Dublin's Human Research Ethics Committee guidelines (under approval LS-E-10-10-Walsh).

### Proteins, Peptides, and Chemicals

Wild-type human A $\beta$ (1–40) (A $\beta$ ), DAEFRHDSGY-EVHHQKLVFF-AEDVGSNKGK-IIGLMVGGVV, A $\beta$  in which serine 26 was substituted with cysteine, and A $\beta$  that contained a N- or C-terminal cysteine and phenylalanine instead

of proline at position 19 were synthesized and purified by Dr. James I Elliott at Yale University (New Haven, CT). Peptide mass and purity (>95%) were confirmed by electrospray ionization/ion trap mass spectrometry and reverse-phase HPLC. Custom-made overlapping A $\beta$  peptide fragments (a Pepset<sup>TM</sup> library) were purchased crude from Mimotopes (Raleigh, NC, USA), and masses confirmed by electrospray mass spectrometry. An immunoglobulin light chain (LC) variable domain  $\lambda_6$  protein, Jto, was produced in *Escherichia coli* and purified as described previously [29]. An anti-A $\beta$  N-terminal mAb, 6E10, was purchased from Signet (Dedham, MA, USA). A polyclonal rabbit anti-A $\beta$  antibody, AW8, was raised against aggregated synthetic A $\beta$ (1–42) and recognizes multiple linear epitopes and can bind to a variety of A $\beta$  conformers [28]. Intravenous immunoglobulin (IVIg; Gammagard liquid<sup>®</sup>) was provided by Baxter BioScience (Vienna, Austria). ImmunoPure Horseradish peroxidase (HRP) and H<sub>2</sub>O<sub>2</sub> (30% in water) were from Pierce (ThermoFisher Scientific, Waltham, MA, USA). Unbranched dextran standards of molecular masses: 43,800; 21,400; 9890, and 4440 were purchased from Pharmacosmos (Holbaek, Denmark). All other chemicals were obtained from Sigma-Aldrich (Saint Louis, MI, USA) and were of the highest purity available.

### Preparation of Amyloidogenic Conformers

WT A $\beta$  monomers, dityrosine cross-linked A $\beta$  protein species (CAPS), disulfide cross-linked S26C A $\beta$  dimers ([S26CA $\beta$ ]<sub>2</sub>), protofibrils formed from [S26CA $\beta$ ]<sub>2</sub> (PFs), and A $\beta$  and LC fibrils were generated as described below, and were used immediately or frozen at –80°C. WT and S26C peptide concentrations were determined by absorbance at 275 nm using the molar extinction coefficient for tyrosine at 275 nm ( $\epsilon_{275} = 1400 \text{ M}^{-1} \cdot \text{cm}^{-1}$ ). The concentrations of CAPS and LC protein were determined using the MicroBCA assay (ThermoFisher Scientific) with a BSA standard curve.

WT and S26C A $\beta$  monomers and [S26CA $\beta$ ]<sub>2</sub> were isolated from different sized A $\beta$  assemblies using size exclusion chromatography (SEC). Peptides were incubated in 50 mM Tris-HCl containing 6 M guanidine HCl, pH 8.0, to dissociate pre-existing aggregates, and then characterized on a HiLoad 16/60 Superdex<sup>TM</sup> 75 column (GE Healthcare Bio-Sciences AB, Uppsala Sweden) eluted at 0.8 ml/min in 25 mM ammonium acetate, pH 8.5 [30]. Fractions that contained A $\beta$  monomers or [S26CA $\beta$ ]<sub>2</sub> were analyzed by SDS-PAGE using 16% polyacrylamide tris-tricine gels and silver staining [31]. Meta-stable Thioflavin T (ThT) positive PFs were generated by diluting freshly-isolated [A $\beta$ 40S26C]<sub>2</sub> to ~0.1 mg/ml in 20 mM sodium phosphate, pH 7.4, and incubating the reaction mixture for ~3 d at 37°C [30]. The reaction was monitored by ThT fluorescence and was judged complete when the fluorescent signal reached a maximum plateau value [32] (Fig. S1A). Formation of protofibrils was confirmed by electron microscopy (EM), and by the presence of ThT positive aggregates in reaction supernatants after centrifugation at 16,000×g for 20 min (Figs. S1B-D & S3).

ThT positive CAPS were generated by incubating ~0.2 mg/ml A $\beta$  for ~3 h at 37°C with 1.1  $\mu\text{M}$  HRP and 250  $\mu\text{M}$  H<sub>2</sub>O<sub>2</sub> in PBS, pH 7.4, and the reaction product purified using copper (CuSO<sub>4</sub>) precipitation [11]. Dityrosine cross-linked peptide was confirmed by SDS-PAGE, ThT and dityrosine fluorescence emission spectra (Figs. S2 & S3). Fluorescence emission was determined with excitation at 320 nm and emission at 350–550 nm, using an Aminco Bowman series 2 spectrofluorimeter.

WT A $\beta$  and LC fibrils were generated by incubating 0.2 mg/ml of the amyloidogenic proteins in PBS containing 0.02% sodium azide, pH 7.4, at 37°C for 14 days [23]. Fibrillogenesis was judged

complete when Thioflavin T (ThT) fluorescence reached maximum plateau values. The reaction products were harvested by centrifugation at 20,200 $\times$ g for 30 min at room temperature, and fibril morphology confirmed by negative contrast EM (Fig. S2).

### TBS Extract of Human Brain

Frozen temporal cortices from 54 and 66 year-old females each with dementia, fulminant amyloid and tangle pathology (Braak stage = x and y, respectively) were obtained from the Dublin Brain Bank ([www.brainbank.ie](http://www.brainbank.ie)). Tris-buffered saline (TBS) extracts of AD brain specimens were prepared, as described previously, divided into 0.3 mL aliquots, and stored at  $-80^{\circ}\text{C}$  [28]. The presence of A $\beta$  in each TBS extract was confirmed using a highly sensitive immunoprecipitation/western blotting protocol and the peptide's concentration estimated by comparison with synthetic A $\beta$  standards [28].

### Isolation of Anti-A $\beta$ NABs

A $\beta$ -reactive NABs were isolated from IVIg using A $\beta$  conformer, LC fibril, or Cibacron blue affinity chromatography [11,17]. A $\beta$  fibril-, CAPS-, or LC fibril-isolated antibodies were generated by passing, at a flow rate of 1 ml/min, 50 ml of 0.22  $\mu\text{m}$  filtered 10 mg/ml IVIg in binding buffer (PBS, pH 7.4) through a fibril or CAPS column consisting of the amyloidogenic conformer cross-linked to N-hydroxysuccinimide (NHS) Sepharose<sup>®</sup>4 fast-flow agarose matrix (Amersham Biosciences Corp., Piscataway, NJ). A $\beta$  monomer-isolated antibodies were generated using an affinity column consisting of an equimolar mix of monomeric N- or C-terminal cysteine containing F19P A $\beta$  cross-linked to iodoacetyl coupling gel (SulfoLink coupling resin, Pierce) [11]. The antibody flow through was collected, and the column washed with binding buffer until the wash solution had no appreciable absorbance at 280 nm. Fibril-bound IgGs were eluted in 1-mL fractions using 0.1 M Glycine-HCl, pH 2.7, into Eppendorf tubes containing neutralization buffer (1 M Tris-HCl, pH 9.0). The concentration of antibody in the eluant and flow through fractions was determined by absorbance at 280 nm using an extinction coefficient of 1.25 and a relative molecular mass of 150,000. Antibody fractions were pooled, buffer exchanged into PBS and concentrated to  $\sim$ 1 mg/ml using a PL-30 Centricon (Millipore) apparatus, used immediately or stored at  $-80^{\circ}\text{C}$ .

Cibacron blue F3GA-isolated IgGs were generated using an Affi-Gel Blue gel column (Bio-Rad Laboratories, Hercules, CA). Briefly, 50 ml of 0.22  $\mu\text{m}$  filtered 20 mg/ml IVIg in binding buffer (PBS containing 0.6 M NaCl, pH 7.4) was passed through the dye column at a flow rate of  $\sim$ 1 ml/min. The column was washed with binding buffer until there was no absorbance at 280 nm, and the dye-bound antibodies eluted using high salt buffer (PBS containing 1.5 M NaCl, pH 7.4). As described above, the concentration of antibody in column fractions was determined by absorbance at 280 nm, and the antibody preparations were pooled, concentrated to 1 mg/ml, and buffer exchanged into PBS.

### Antibody Binding to Amyloidogenic Conformers

Our standard ELISAs [33], europium-linked immunosorbent microtiter plate assay [23], and immunoprecipitation (IP)/Western blot protocol [34] were used to establish NAB and control antibody's interactions with synthetic A $\beta$  conformers, LC fibrils, and AD brain-derived A $\beta$ . Antibody binding to microtiter plate-immobilized amyloidogenic conformers (400 ng/well) was carried out in the presence or absence of solution-phase A $\beta$  inhibitors in assay buffer consisting of PBS containing 1% BSA and 0.05% Tween 20, pH 7.4. A biotinylated polyclonal goat anti-human or anti-mouse IgG ( $\mu$  heavy chain specific; Jackson ImmunoResearch

Laboratories, Inc., West Grove, PA, USA) served as the secondary antibody. Streptavidin-HRP (Jackson ImmunoResearch Laboratories, Inc.) and TMB substrate (SureBlue Reserve<sup>™</sup>; KPL, Gaithersburg, MD, USA), or streptavidin-europium and enhanced solution (DELIA<sup>®</sup>; PerkinElmer, Inc., Boston, MA, USA) served as the detection system. Antibody binding to solution-phase amyloidogenic conformers was determined using a capture ELISA consisting of plate-immobilized antibody ( $\sim$ 400 ng/well) binding to synthetic A $\beta$  conformers in assay buffer. A polyclonal rabbit anti-A $\beta$  antibody, AW8 [28] served as the secondary antibody, and a HRP-conjugated donkey anti-rabbit IgG (whole molecule, GE Healthcare, Buckinghamshire, UK) and TMB substrate (SureBlue Reserve<sup>™</sup>; KPL) were used as the detection system.

Immunoprecipitation/Western blot analysis of solution-phase antibody binding to synthetic A $\beta$  conformers and AD brain-derived A $\beta$  was investigated using samples that were precleared for nonspecific protein binding to the antibody capture beads (a 1:1 mixture of Protein A sepharose (Sigma) and Protein G agarose (Roche, Mannheim, Germany)) [34]. Briefly, 0.5 ml of neat TBS extract of AD or normal brain, or the same volume of a synthetic A $\beta$  conformer (diluted to  $\sim$ 0.2–20  $\mu\text{g}/\text{ml}$  with 1% BSA in PBS containing 0.05% Tween, pH 7.4), was incubated with 20  $\mu\text{l}$  of antibody capture beads for 1 h at room temperature. The beads were sedimented by centrifugation at 4,000 $\times$ g for 5 min, the supernatant collected, IVIg (100  $\mu\text{g}/\text{ml}$ ) or AW8 (200  $\mu\text{g}/\text{ml}$ ) added to the precleared samples, and the mixtures incubated as before. The antibody-bead complexes were sedimented, supernatants removed, pellets washed, and antibody-bound A $\beta$  liberated by heating the pellet at  $100^{\circ}\text{C}$  for 5 min in 2 $\times$ SDS sample buffer [34]. The boiled samples were immediately electrophoresed on 16% polyacrylamide tris-tricine gels, transferred onto 0.2  $\mu\text{m}$  nitrocellulose (Optitran, Schleicher and Schull, Germany) at 400 mA for 2 h. Membrane-bound A $\beta$  was then detected using an equimolar mixture (0.5  $\mu\text{g}/\text{ml}$  each) of N-terminal and mid-region A $\beta$ -reactive mAbs 6E10 and 4G8, and enhanced chemiluminescence (Thermo Fisher Scientific Inc, Rockford, IL) as the detection system [34].

### Thioflavin T Fluorescence

Fluorescent measurements were carried out in duplicate by diluting an A $\beta$  or LC sample to 3  $\mu\text{g}/100 \mu\text{l}/\text{well}$  with assay buffer (PBS, pH 7.4, or 25 mM ammonium acetate, pH 8.5, containing 30  $\mu\text{M}$  ThT) in a black polystyrene 96-well microtiter plate (ThermoFisher Scientific). ThT signal was determined with excitation at 435 nm and emission at 485 nm using a SpectraMax M2 multi-detection microplate reader (Molecular Devices Corp., Sunnyvale, CA) [35].

### Electron Microscopy

Negative contrast EM was performed by applying 10  $\mu\text{l}$  aliquots of a test sample on to duplicate carbon-coated formvar grids (Electron Microscope Sciences, Washington, PA) that were cross-linked with 0.5% (v/v) glutaraldehyde, and stained with 2% (w/v) uranyl acetate solution (Ted Pella, Inc., Redding, CA). The EM grids were examined using a Tecnai<sup>™</sup> G<sup>2</sup> Spirit BioTWIN electron microscope (FEI, Hillsboro, OR).

### Circular Dichroism Spectroscopy

A $\beta$  solutions ( $\sim$ 0.2 mg/ml) were placed in a 1 mm path length quartz cuvette (Starna Scientific Ltd., Essex, UK) and spectra obtained at  $22^{\circ}\text{C}$  using a J-810 JASCO spectropolarimeter (JASCO Corp., Tokyo, Japan) [30]. Spectra were generated from three data accumulations between  $\sim$ 195–260 nm with 10 nm/min continuous scanning and a 0.5 nm bandwidth. Raw data were

manipulated by subtraction of buffer spectra and by binomial smoothing according to the manufacturer's instructions (JASCO Corp.).

### General Curve Fitting

Antibody binding curves and aggregation time courses were fitted using SigmaPlot 2000, version 6 (Systat Software, Chicago, IL) or GraphPad Prism, version 5 (GraphPad Software, Inc., La Jolla, CA, USA).

## Results

### NABs Primarily Recognize A $\beta$ -related Conformational Epitope(s)

NAB's preference for conformational or linear sequence epitopes on A $\beta$  was determined by ELISA and affinity column chromatography using as substrates, A $\beta$  conformers (monomers, CAPS, fibrils) and non-A $\beta$  fibrils that consisted of LC protein with no known primary sequence identity with A $\beta$ . The antibody binding curves and column depletion studies shown in Figure 1 demonstrate that the majority, if not all, of NAB's binding to A $\beta$  was directed against conformational epitope(s) that were similarly exposed on LC fibrils. In particular, NABs isolated from IVIg after one passage through an A $\beta$  or LC fibril column recognized either fibril species, but had a slight (~3-fold) preference for the plate-immobilized fibril that the antibodies were purified against, with antibody concentration at half maximal effect, EC<sub>50</sub>, of ~40 nM (Fig. 1A–D, Table 1). In contrast, anti-A $\beta$  NABs isolated and pooled from four sequential passages of an IVIg preparation through either fibril column (eluant and flow through generated for each passage) had similar reactivity with plate-immobilized A $\beta$  fibrils and LC fibrils, with EC<sub>50</sub> values of ~60 nM. The antibody flow through from the fourth passage for each column was similarly depleted (~80–100%) against binding to A $\beta$  conformers (monomers, CAPS, fibrils) and LC fibril column matrices, even though the preparations still contained ~99% of antibodies that were originally applied to the columns (Fig. 1E–F). SDS-PAGE analysis confirmed that the antibody eluants had no detectable A $\beta$  or LC that may have leaked off the affinity matrices.

The NAB's reliance on A $\beta$ 's conformational state, and not a particular linear sequence segment, was confirmed by A $\beta$  fibril-isolated Nab's nM binding to plate-immobilized A $\beta$  fibrils, and only weak  $\mu$ M reactivity with monomers and overlapping peptide fragments of the 40- and 42-mer A $\beta$  peptides (Fig. 2). The anti-A $\beta$  NABs bound ~40-fold stronger to plate-immobilized A $\beta$  fibrils than control NABs from an A $\beta$  fibril column flow through preparation. Notably, both the anti-A $\beta$  NAB and antibody flow through preparations had similar  $\mu$ M avidity for plate-immobilized A $\beta$  monomers and peptide fragments, indicating that these interactions were nonspecific. The NAB's relatively weak interactions with A $\beta$  monomers was not due to an antibody-bound antigen masking A $\beta$  reactivity since pretreating the NAB's to dissociate such complexes, using a low pH (3.5) method [36], only enhanced antibody reactivity ~2-fold against plate-immobilized A $\beta$  monomers (Fig. S4). Moreover, the antibodies had enhanced binding to the ELISA blocking agent, BSA, compared to untreated NABs, indicating that acid pretreatment induced non-specific IgG polyreactivity. In contrast to NABs, a control anti-A $\beta$  N-terminal mAb, 6E10, bound similarly to plate-immobilized A $\beta$  fibrils, and N-terminal A $\beta$  fragments, A $\beta$ (1–15) and A $\beta$ (3–13) (Fig. 2).

Given the Nab's propensity to cross-react with A $\beta$  and LC aggregates [17], we established if these antibody's still maintained binding to A $\beta$  conformers in the presence of normal human plasma and CSF – bodily fluids which contain endogenous

molecules that bind to amyloidogenic assemblies [37]. Figure 3 and Table 2 show that normal human plasma had only a modest effect on NAB binding to plate-immobilized CAPS and A $\beta$  fibrils. Plasma reduced the maximum binding signal amplitude by ~40%, but did not affect strong antibody-fibril interactions since at relatively low antibody concentrations, depicted by the sloping segments of the binding curves, the fluid had no effect. Plasma's net effect was to lower EC<sub>50</sub> values for NABs binding to plate-immobilized CAPS and A $\beta$  fibrils by ~3-fold, with EC<sub>50</sub> values of ~30 nM (Fig. 3, Table 2). In contrast, CSF had no effect on NAB binding to A $\beta$  (data not shown).

### Anti-A $\beta$ NABs can be Isolated by Cibacron Blue Affinity Chromatography

Pursuant to using Cibacron blue F3GA to remove albumin from plasma, we discovered that under high salt conditions, anti-A $\beta$  NABs bound specifically to this dye. Figure 4 and Table 3 show that anti-A $\beta$  NABs isolated by passing IVIg through a Cibacron blue column bound ~20-fold stronger to plate-immobilized A $\beta$  fibrils and CAPS than the unfractionated preparation, with EC<sub>50</sub>s of ~100 nM. In contrast, the same preparation was only ~2-fold enriched in binding to plate-immobilized A $\beta$  monomers, with EC<sub>50</sub>s of ~500 nM (Fig. 4, Table 3). Essentially no anti-A $\beta$  IgGs were isolated using the bead matrix alone, confirming that the antibodies bound specifically to the dye. The relatively high ionic strength required to facilitate anti-A $\beta$  NABs binding to Cibacron blue suggests that dye-NAB complexes were stabilized by hydrophobic interactions. However, we were not able to specifically isolate anti-A $\beta$  IgGs from IVIg using a standard hydrophobic matrix, phenyl sepharose CL-4B (Sigma). The amount of antibody that eluted off the dye column after one passage, determined by absorbance at 280 nm, corresponded to ~0.6% of the total IgGs applied, and was ~3-fold more than was obtained using a similarly sized A $\beta$  fibril column. The relatively large amount of dye-isolated antibodies presumably reflected a greater proportion of A $\beta$ -unreactive antibodies than was present in A $\beta$  fibril-isolated antibody preparations, and resulted in a ~2-fold larger EC<sub>50</sub> value of ~100 nm for dye-isolated NABs binding to plate-immobilized A $\beta$  aggregates (Fig. 4, Table 3). Despite the latter differences, two experimental findings indicate that the dye- and fibril-isolated antibody preparations contained similar anti-A $\beta$  IgGs. First, four sequential passages of an IVIg preparation through either the dye or fibril column (eluant and flow through generated for each passage) removed ~1% of the antibodies that were originally applied to the column, but the final antibody flow through was >90% reduced in binding to an A $\beta$  fibril column. Lastly, both the dye- and A $\beta$  fibril-isolated IgGs were similarly cross-reactive with A $\beta$  and LC fibrils (Fig. 4D, Table 3).

### NABs Recognize Synthetic A $\beta$ Dimer Assemblies and AD Brain-derived A $\beta$

An array of A $\beta$  assemblies are likely to mediate toxicity, but burgeoning evidence suggests that water-soluble non-fibrillar assemblies, including those formed from A $\beta$  dimers, have disease-relevant activity [4,25,30,38]. Consequently, we investigated NABs ability to bind to soluble A $\beta$  dimer assemblies by ELISA and immunoprecipitation/Western blot analyses using synthetic [S26CA $\beta$ ]<sub>2</sub> and synaptotoxic PFs formed from [S26CA $\beta$ ]<sub>2</sub> [30,38]. Anti-A $\beta$  NABs used in these studies were isolated by Cibacron blue and not by fibril affinity chromatography since a very small amount of A $\beta$  was identified in A $\beta$  fibril-isolated antibody preparations (~0.2  $\mu$ g/ml A $\beta$  (46 nM w.r.t. monomers) in ~2 mg/ml antibody samples) using a highly

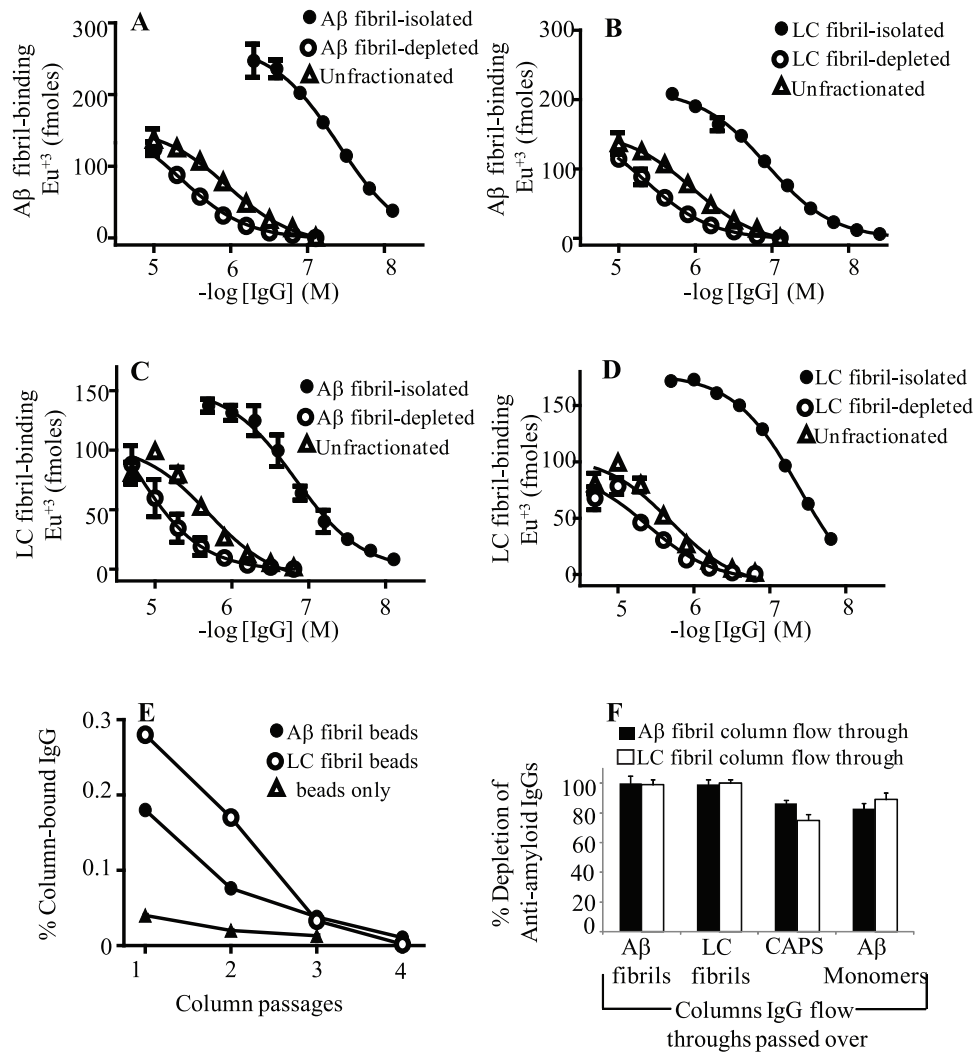


**Figure 1. A $\beta$  and LC fibril fractionated NAb binding to amyloid fibrils.** The antibody binding curves are for A $\beta$  fibril (A) and LC fibril (B) fractionated IVIg against plate-immobilized A $\beta$  fibrils, and for A $\beta$  fibril- (C) and LC fibril- (D) isolated IVIg IgGs against plate-immobilized LC fibrils. Each data point represents the average value from three binding studies, which were carried out using assay buffer consisting of 1% BSA in PBS containing 0.05% tween 20, pH 7.4. (E) The % IgGs isolated for each of four sequential passages of a preparation of 10 mg/ml IVIg in PBS, pH 7.4, through a column consisting of A $\beta$  or LC (○) fibrils covalently cross-linked to N-hydroxysuccinimide (NHS) Sepharose®4 fast-flow agarose matrix (Amersham Biosciences Corp.). The plots also show the % IgGs isolated from IVIg over a control unconjugated deactivated sepharose matrix (beads only). The concentration of antibody in eluant preparations was determined by absorbance at 280 nm using an extinction coefficient of 1.25 and a relative molecular mass of 150,000. (F) The % depletion of anti-amyloidogenic NAb in IVIg flow through preparations from A $\beta$  and LC fibril columns, respectively, compared to the unfractionated preparation. Each antibody flow through preparation was generated from the fourth passage of IVIg through a fibril column, as described in Panel E (IgG eluant and flow through was generated for each passage). The % depletion of A $\beta$  conformer and LC fibril reactive NAb in each antibody flow through was determined from the absorbances at 280 nm of antibody eluants generated by passing IVIg and the antibody flow through preparations through A $\beta$  conformer or LC fibril columns. doi:10.1371/journal.pone.0050317.g001

sensitive immunoprecipitation/Western blot protocol [34]. The contaminating peptide was only sufficient to bind to ~0.4% of the fibril-isolated NAb (assuming 1:1 interactions of A $\beta$  with IgG), and did not sufficiently affect ELISA determination of antibody avidity, but was sufficient to compromise immunoprecipitation/Western blot investigations.

The SEC chromatograph shown in Figure 5 indicates that freshly-isolated [S26CA $\beta$ ]<sub>2</sub> were highly pure, and based on the use of linear dextran standards, had an apparent molecular weight of ~10 kDa. A portion of the conformer migrated as a ~16 kDa assembly in denaturing SDS-PAGE, but this was transiently and artificially induced by the detergent [30,39]. The dye-isolated NAb bound >10-fold stronger to plate-immobilized [S26CA $\beta$ ]<sub>2</sub>

and PFs than to WT A $\beta$  monomers, with EC<sub>50</sub>s of ~50–100 nM (Fig. 5, Table 4). In contrast, mAb, 6E10 did not have a preference for any of the plate-immobilized A $\beta$  conformers (Table 4).

Since surface-adsorption of A $\beta$  can artificially induce amyloid-like epitopes [11,40], we also tested if the NAb could bind to [S26CA $\beta$ ]<sub>2</sub> and PFs in solution. Panel E of Figure 5 and Table 4 show that plate-immobilized anti-A $\beta$  NAb captured solution-phase [S26CA $\beta$ ]<sub>2</sub> and PFs, with EC<sub>50</sub> values of ~5–10  $\mu$ g/ml (0.6–1.2  $\mu$ M w.r.t. the dimeric peptide). In contrast, the antibodies bound much weaker to WT A $\beta$  monomers (EC<sub>50</sub>>100  $\mu$ g/ml). NAb's preference for aggregated A $\beta$  was not an artifact induced by the secondary anti-A $\beta$  polyclonal antibody, AW8, used in the capture ELISA since AW8 bound similarly to saturating amounts

**Table 1.** Unmodified and A $\beta$  and LC fibril-isolated NABs binding to plate-immobilized amyloid fibrils.

IVIg	A $\beta$ fibrils		LC fibrils		
	EC <sub>50</sub> <sup>1</sup>	Max signal <sup>1</sup>	EC <sub>50</sub>	Max signal	EC <sub>50</sub> A $\beta$ fibrils
	(nM)	Eu <sup>+2</sup> (fm)	(nM)	Eu <sup>+2</sup> (fm)	EC <sub>50</sub> LC fibrils
Unfractionated	1012 $\pm$ 74	146 $\pm$ 3.4	2000 $\pm$ 24	92 $\pm$ 6.5	0.50
A $\beta$ fibril enriched	38 $\pm$ 0.2	263 $\pm$ 5.3	137 $\pm$ 0.9	147 $\pm$ 5.4	0.28
A $\beta$ fibril residual	~3000	>100	~5000	>90	-
LC fibril enriched	122 $\pm$ 0.7	215 $\pm$ 6.8	52 $\pm$ 0.1	175 $\pm$ 1.8	2.3
LC fibril residual	2884 $\pm$ 11	133 $\pm$ 2.4	3251 $\pm$ 58	77 $\pm$ 8.6	0.89

<sup>1</sup>Each value for EC<sub>50</sub> and max signal for NAb binding to plate-immobilized A $\beta$  or LC fibrils was the average value obtained from three sigmoidal fitted antibody binding curves, such as shown in Figure 1.

doi:10.1371/journal.pone.0050317.t001

of PFs or WT monomers bound to plate-immobilized anti-A $\beta$  NABs (data not shown). Solution-phase competition ELISA studies, where both NAb and A $\beta$  conformers were in solution, further verified the antibody's preference for aggregated A $\beta$ . Figure 5F and Table 4 show that [S26CA $\beta$ ]<sub>2</sub> and PFs dose-dependently inhibited antibody binding to plate-immobilized [S26CA $\beta$ ]<sub>2</sub>, with inhibitor concentrations at half maximal effect, IC<sub>50</sub> values, of ~4 and 16  $\mu$ g/ml (~0.5 and 1.8  $\mu$ M w.r.t. the dimeric peptide), respectively. In contrast, WT A $\beta$  monomers lacked significant inhibitory activity, with IC<sub>50</sub> values >50  $\mu$ g/ml (>11.6  $\mu$ M) (Fig. 5, Table 4). To verify NAb binding to A $\beta$  conformers in solution, we tested their ability to immunoprecipitate various synthetic A $\beta$  assemblies. Consistent with our ELISA

results, Figure 6A shows that the NABs preferentially bound to [S26CA $\beta$ ]<sub>2</sub> and PFs without detectable binding to the monomeric peptide. In contrast mAb 6E10 similarly immunoprecipitated all A $\beta$  conformers (Fig. 6A). Control experiments confirmed that the A $\beta$  aggregates did not significantly bind to the protein A/G matrix alone.

Having demonstrated nM binding by NABs to synthetic A $\beta$  dimer assemblies, we established if they could recognize A $\beta$  from the water-soluble phase of AD brain [34]. Figure 6B shows that the anti-A $\beta$  NABs and our control polyclonal anti-A $\beta$  antibody, AW8, immunoprecipitated A $\beta$  (<1 and >5 ng/ml, respectively) that was present in TBS extracts of two AD brains, but had no reactivity with TBS extract of a normal age-

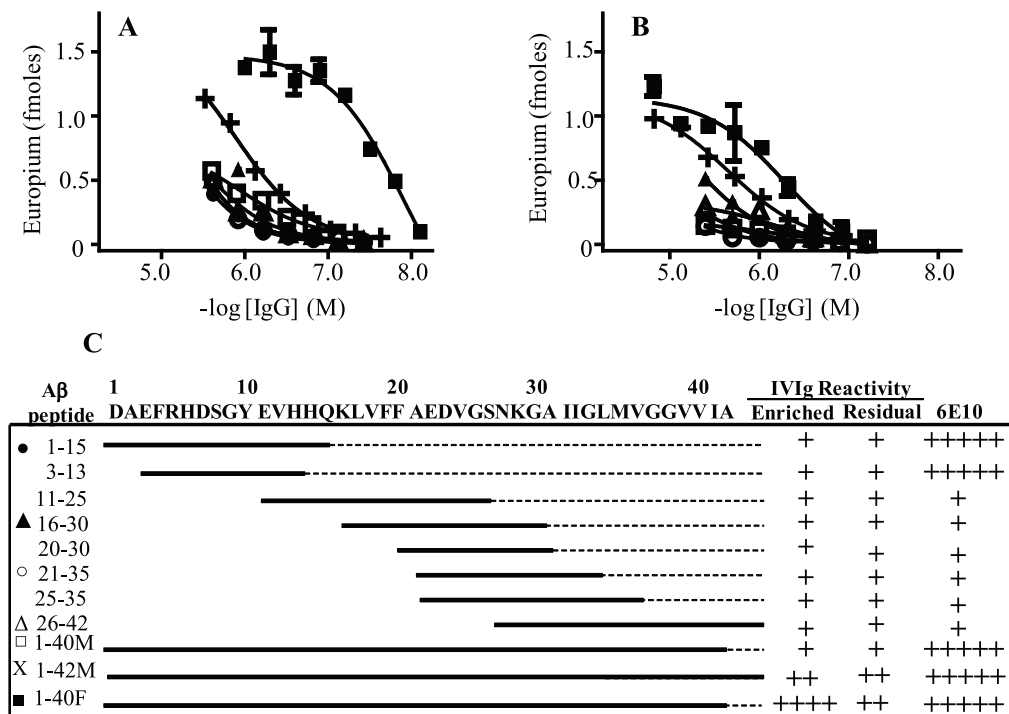


**Figure 2. NABs binding to A $\beta$  conformers and overlapping peptide fragments.** The antibody binding curves are representative of A $\beta$  fibril-isolated (A) and column flow through (depleted) (B) IVIg fractions against plate-immobilized A $\beta$  conformers and overlapping A $\beta$  peptide fragments, respectively. The data symbols represent antibody binding to the A $\beta$  peptides specified in Panel C. (C) Schematic comparison of A $\beta$  fibril-isolated and flow through IVIg fractions, as well as an anti-A $\beta$  N-terminal mAb, 6E10, binding to the plate-immobilized A $\beta$  conformers and overlapping peptide fragments.

doi:10.1371/journal.pone.0050317.g002

**Table 2.** Plasma inhibition of NAb binding to A $\beta$  conformers.

A $\beta$ conformer	No plasma		+ Plasma		Plasma alone	
	EC <sub>50</sub> <sup>1</sup>	Max signal <sup>1</sup>	EC <sub>50</sub>	Max signal	EC <sub>50</sub>	Max signal
	(nM)	Eu <sup>+2</sup> (fm)	(nM)	Eu <sup>+2</sup> (fm)	(nM)	Eu <sup>+2</sup> (fm)
Fibrils	67 $\pm$ 1	232 $\pm$ 15	26 $\pm$ 0.4	121 $\pm$ 10	350 $\pm$ 0.6	26 $\pm$ 4
CAPS	62 $\pm$ 0.2	263 $\pm$ 5.3	21 $\pm$ 0.1	132 $\pm$ 4.0	341 $\pm$ 1.5	54 $\pm$ 2

<sup>1</sup>Each value for EC<sub>50</sub> and max signal for anti-A $\beta$  NAb, isolated from IVIg using A $\beta$  fibril affinity chromatography, binding to plate-immobilized A $\beta$  fibrils and CAPS was the average value obtained from three sigmoidal fitted antibody binding curves, such as shown in Figure 3. doi:10.1371/journal.pone.0050317.t002

matched control brain. Control experiments confirmed that the antibodies and not protein A/G beads alone bound to AD brain-derived A $\beta$  (Fig. 6B). The immunoprecipitated A $\beta$  peptide migrated in denaturing SDS-PAGE as monomers and dimers. Whether the immunoprecipitated A $\beta$  actually existed in solution under native conditions as monomers and dimers is uncertain since we have previously shown that A $\beta$  derived from human brain elutes from SEC with a range of molecular weights, but that when subjected to SDS-PAGE only monomers and dimers are detected [38]. We take these results to mean that A $\beta$  from the aqueous phase of human brain can exist in different sized assemblies, built up of A $\beta$  monomer and/or SDS-stable A $\beta$  dimer (for discussion see [30]), and that the NAb did not recognize authentic A $\beta$  monomers, but larger A $\beta$  assemblies.

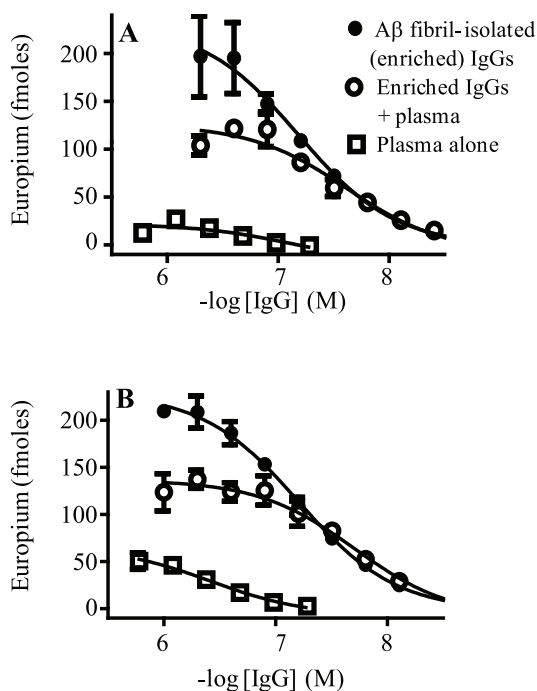


**Figure 3. Plasma inhibition of NAb binding to A $\beta$  conformers.** The antibody binding curves show A $\beta$  fibril-isolated IVIg IgGs binding to plate-immobilized A $\beta$  fibrils (A) and CAPS (B) in the absence or presence of a 1:10 dilution of normal human plasma. The plots also show A $\beta$  conformer binding by plasma IgGs alone. The data symbols in Panels A and B represent A $\beta$  conformer binding by antibody preparations as specified in the legend of Panel A. doi:10.1371/journal.pone.0050317.g003

## Discussion

Anti-A $\beta$  immunotherapy is a promising approach for AD, and increasing experimental evidence indicates that soluble A $\beta$  aggregates, including assemblies formed from dimers, are the primary toxic species [5,6,26,30,41]. IVIg, which contains anti-A $\beta$  NAb, has shown promise in recent clinical trials for AD, but its mode of action is not yet known [12,13]. Nevertheless, current research is primarily focused on anti-A $\beta$  NAb since extensive *in vitro* and transgenic animal studies have indicated that these antibodies have unique therapeutic potential for AD [11,12,16,17,18,19,20]. Our finding that anti-A $\beta$  NAb have nM avidity for solution-phase synthetic A $\beta$  dimer assemblies and AD brain-derived A $\beta$ , as well as their ability to recognize soluble synthetic cross-linked  $\beta$ -amyloid protein species (CAPS) [11] and A $\beta$  trimers [18], indicates that these antibodies are, at least in part, responsible for IVIg's modulation of AD patient's levels of cerebral and blood pool soluble A $\beta$  [12,13,18]. In particular, infusions of IVIg have reduced patient's cerebral A $\beta$  and concurrently increased A $\beta$ 's blood pool – a process consistent with the beneficial effects of anti-A $\beta$  immunotherapy [5,6]. Notably, Dodel's lab have recently shown that vaccinating AD transgenic mice with anti-A $\beta$  NAb, which were isolated from IVIg using an A $\beta$  affinity column, reduced cerebral A $\beta$  levels, increased the peptide's blood pool, and significantly improved the animal's object location memory [18].

Anti-A $\beta$  NAb-mediated clearance of cerebral A $\beta$  may occur through several, not mutually exclusive, mechanisms. This includes Fc-mediated clearance, rapid efflux of A $\beta$  to the periphery via antibody-A $\beta$  complexes, antibody inhibition of A $\beta$  aggregation, and a peripheral sink mechanism whereby antibody targeting of blood pool A $\beta$  alters an equilibrium between brain and blood pool A $\beta$  that causes an efflux of the peptide into the periphery [42,43]. Our findings suggest that the latter peripheral sink mechanism is the most plausible mode of action for anti-A $\beta$  NAb since their modest (nM) avidity for solution-phase A $\beta$  aggregates may be offset by their relatively high concentration in the blood. In contrast, NAb binding to cerebral A $\beta$  is likely to be minimal since only  $\sim$ 0.1% of these antibodies may enter the brain [44]. Furthermore, our demonstration that NAb binding in plasma indicates that they are not significantly inhibited from reacting with peripheral A $\beta$  by endogenous plasma molecules [37]. Alternatively, IVIg's modulation of A $\beta$  in bodily fluids of AD patient and transgenic mice may not be due to NAb's modulation of an equilibrium between cerebral and blood pool A $\beta$ , but their direct clearance of A $\beta$  in the brain, and peripheral NAb binding to blood pool A $\beta$ , which in itself can increase the peptide's half-life [42,45]. Levels of cerebral A $\beta$  may have also been reduced by NAb in IVIg that can target a receptor for advanced glycation end

**Table 3.** Unfractionated, Cibacron blue- and A $\beta$  fibril-isolated NAbs binding to plate-immobilized amyloidogenic conformers.

Conformer	Unfractionated		Cibacron blue-isolated		A $\beta$ Fibril-isolated	
	EC <sub>50</sub> <sup>1</sup>	Max signal	EC <sub>50</sub>	Max signal	EC <sub>50</sub>	Max signal
	(nM)	Eu <sup>+2</sup> (fm)	EC <sub>50</sub>	Eu <sup>+2</sup> (fm)	(nM)	Eu <sup>+2</sup> (fm)
A $\beta$ Fibrils	927 $\pm$ 5	89 $\pm$ 4	105 $\pm$ 1	131 $\pm$ 8	45 $\pm$ 1	133 $\pm$ 4
CAPS	~3000	>100	120 $\pm$ 2	168 $\pm$ 6	62 $\pm$ 0.3	226 $\pm$ 4
A $\beta$ Monomers	~1000	>15	542 $\pm$ 4	82 $\pm$ 1	547 $\pm$ 1	106 $\pm$ 2
LC fibrils	2160 $\pm$ 20	35 $\pm$ 2	46 $\pm$ 1	43 $\pm$ 2	20 $\pm$ 1	61 $\pm$ 3

<sup>1</sup>Each value for EC<sub>50</sub> and max signal for A $\beta$ -reactive NAbs binding to a plate-immobilized amyloidogenic conformer was determined from the average value obtained from three sigmoidal fitted antibody binding curves, such as shown in Figure 4.  
doi:10.1371/journal.pone.0050317.t003

products (RAGE) [46], a protein that transports A $\beta$  into the brain [47], and/or soluble low-density lipoprotein receptor-related protein-1 (sLRP1) [48], a major A $\beta$  binding protein in the blood that is present in IVIg [46].

The proximate pathogenic A $\beta$  specie(s) to target are still unknown, but assemblies formed from A $\beta$  dimers are prime candidates [26,30,33,38]. The NAbs nM avidity for synthetic A $\beta$  dimer assemblies, [S26CA $\beta$ ]<sub>2</sub> and synaptotoxic PFs, and AD brain-derived A $\beta$  suggests that these antibodies recognize the pathogenic peptide [30,38]. As mentioned above, although NAbs can immunoprecipitate AD brain-derived A $\beta$ , their modest avidity for these conformers, and inability to penetrate the blood brain barrier, suggests that these antibodies are more likely to target A $\beta$  in the periphery, such as plasma membrane-bound A $\beta$  dimers [27]. Nevertheless, anti-A $\beta$  antibodies that enter the brain may still benefit an AD patient by clearing A $\beta$  to the periphery, and/or by neutralizing toxic A $\beta$  species [8,16,18,21] (Fig. S5).

The conformational A $\beta$  epitope(s) recognized by NAbs presumably consist of sequentially discontinuous segments that are close together in three-dimensional space [49]. Our observation that these surfaces are similarly exposed on A $\beta$  aggregates and LC fibrils is consistent with our previous observations that NAbs can react with aggregated A $\beta$  and are pan amyloid fibril-reactive [11,17]. Such epitopes may be formed from A $\beta$ -A $\beta$  interactions, or could also be generated *in vivo* from the interaction of monomeric peptide with endogenous molecules or matrices [11,40]. The inability of NAbs to recognize synthetic A $\beta$  monomers or the fragmented peptide contrasts with previous studies that suggested anti-A $\beta$  NAbs specifically recognize linear sequence segments (for example [18,19,50]). However, the latter studies primarily involved surface-immobilized synthetic A $\beta$ , which due to surface adsorption can artificially expose amyloidogenic epitopes that are not present on the solution-phase native peptide [11]. Also, NAb binding to A $\beta$  was not compared to

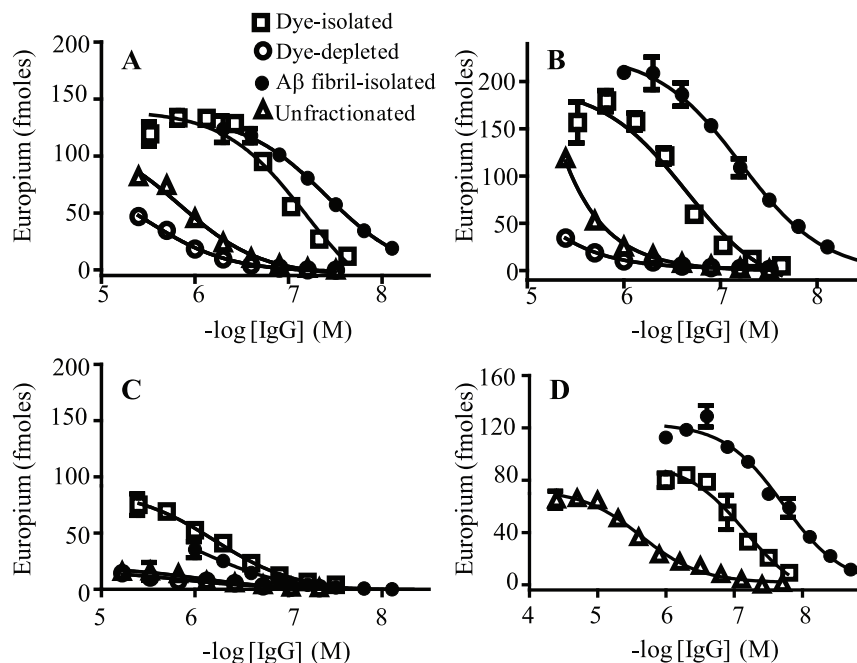


**Figure 4. Cibacron blue and A $\beta$  fibril fractionated NAbs binding to amyloidogenic conformers.** Antibody binding curves were generated for unfractionated IVIg, Cibacron blue-isolated and depleted, and for A $\beta$  fibril-isolated IVIg IgGs against plate-immobilized A $\beta$  fibrils (A), CAPS (B), A $\beta$  monomers (C), and LC fibrils (D). The data symbols in Panels A to D represent A $\beta$  conformer binding by antibody preparations as specified in the legend of Panel A.  
doi:10.1371/journal.pone.0050317.g004



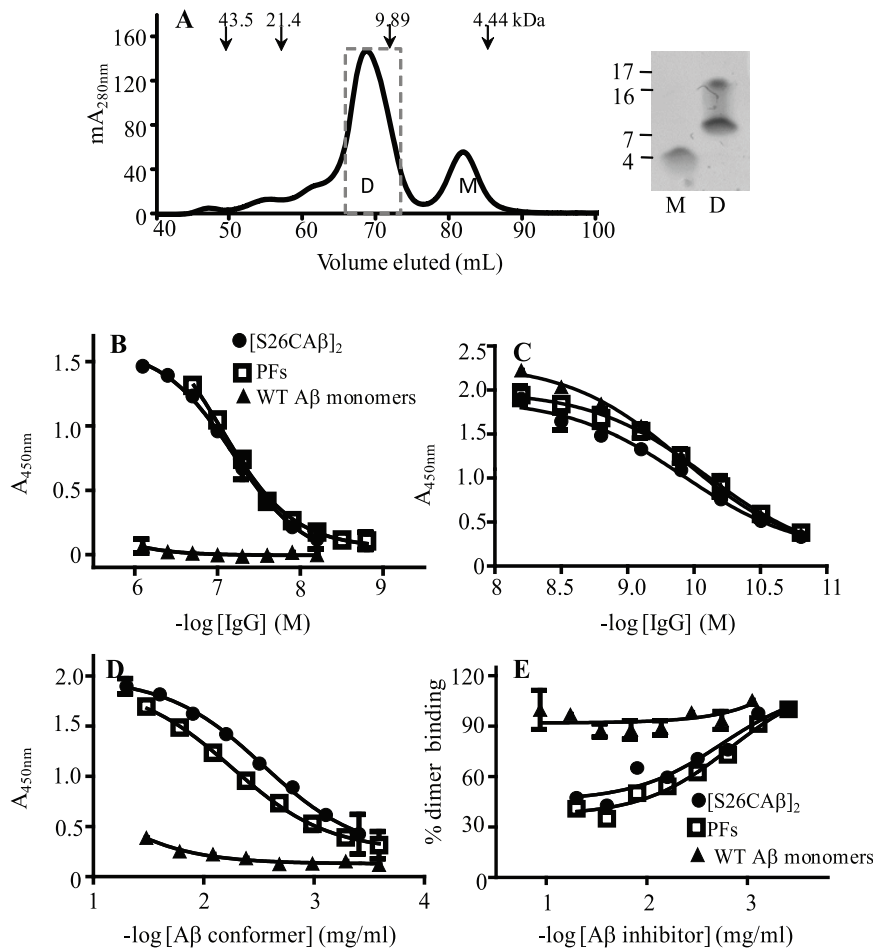


**Figure 5. Isolation of A $\beta$  dimers and NAb binding.** (A) [S26CA $\beta$ ]<sub>2</sub> was isolated by SEC using a HiLoad 16/60 Superdex 75 column equilibrated with 25 mM ammonium acetate, pH 8.5. Arrows indicate elution of linear dextran standards, and D and M are abbreviations for A $\beta$  dimers and monomers, respectively. SDS-PAGE analysis of the low molecular weight SEC peaks confirmed the presence of dimers or monomers. A portion of A $\beta$  in the dimer fraction migrated as an ~16 kDa assembly that was transiently and artificially induced by the detergent [30,39] (B) Cibacron blue-isolated IVIg, (C) anti-A $\beta$  N-terminal mAb, 6E10, binding to plate-immobilized A $\beta$  conformers: [S26CA $\beta$ ]<sub>2</sub>, PFs, and WT A $\beta$  monomers. (D) Plate-immobilized Cibacron blue-isolated IVIg binding to solution-phase A $\beta$  conformers, and (E) A $\beta$  competition curves for solution-phase A $\beta$  conformer inhibition of 100 nM Cibacron blue-isolated IVIg binding to plate-immobilized [S26CA $\beta$ ]<sub>2</sub>. The data symbols in Panels B to E represent antibody binding to A $\beta$  conformers as specified in the legend of Panel B. doi:10.1371/journal.pone.0050317.g005

**Table 4.** Unfractionated and Cibacron blue-isolated NABs binding to plate-immobilized amyloidogenic conformers.

A $\beta$ Conformer	Direct ELISA				CB <sup>1</sup> -isolated IVIg		
	CB-isolated IVIg		mAb 6E10		A $\beta$ capture	A $\beta$ comp	
	EC <sub>50</sub> <sup>2</sup> (nM)	Max <sup>3</sup> A <sub>450nm</sub>	EC <sub>50</sub> (nM)	Max A <sub>450nm</sub>	EC <sub>50</sub> ( $\mu$ g/ml)	Max A <sub>450nm</sub>	IC <sub>50</sub> <sup>2</sup> ( $\mu$ g/ml)
[S26CA $\beta$ ] <sub>2</sub> PFs	64 $\pm$ 2	1.6 $\pm$ 0.1	0.12 $\pm$ 0.01	2.0 $\pm$ 0.1	4.4 $\pm$ 0.02	1.9 $\pm$ 0.01	4.4 $\pm$ 0.02
[S26CA $\beta$ ] <sub>2</sub> dimers	105 $\pm$ 2	~1.50	0.09 $\pm$ 0.01	2.1 $\pm$ 0.1	9.9 $\pm$ 0.3	1.9 $\pm$ 0.02	16 $\pm$ 0.01
CAPS	50 $\pm$ 1	1.3 $\pm$ 0.1	0.15 $\pm$ 0.02	2.2 $\pm$ 0.02	12 $\pm$ 0.3	1.6 $\pm$ 0.01	>50
WT monomers	>800	–	0.12 $\pm$ 0.01	2.4 $\pm$ 0.01	>100	–	>100

<sup>1</sup>CB is an abbreviation for Cibacron blue.

<sup>2</sup>Each value for EC<sub>50</sub>, max signal, and IC<sub>50</sub> for antibody binding to a plate-immobilized A $\beta$  conformer was the average value obtained from three sigmoidal fitted antibody binding curves, such as shown in Figure 5.

<sup>3</sup>Max is an abbreviation for maximum assay signal.

doi:10.1371/journal.pone.0050317.t004

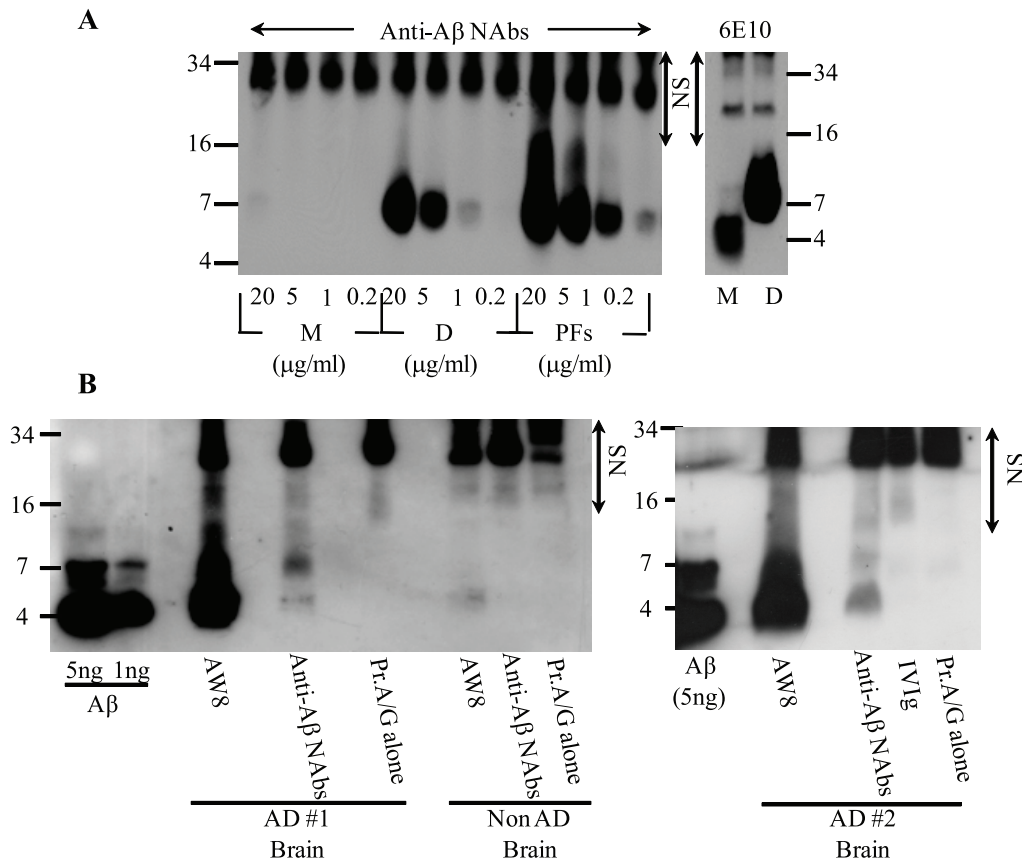


**Figure 6. NAb immunoprecipitation of synthetic and AD brain-derived A $\beta$ .** (A) Western blot analysis of synthetic S26CA $\beta$  conformers immunoprecipitated by NAbs isolated from IVIg by Cibacron blue affinity chromatography, and by mAb 6E10: M, monomers; D, dimers, and PFs. (B) Western blot analysis of soluble A $\beta$  present in TBS extracts of AD brain immunoprecipitated by unfractionated and Cibacron blue-isolated IVIg IgGs, and by rabbit polyclonal anti-A $\beta$  IgGs, AW8. Prot A/G alone stands for control studies carried out with antibody capture beads (a 1:1 mixture of Protein A sepharose and Protein G agarose) and brain extract without primary antibody. The Western blots were developed using N-terminal and mid-region A $\beta$ -reactive mAbs, 6E10 and 4G8, and enhanced chemiluminescence as the detection system. NS, indicates non-specific bands arising from secondary antibody detection of NAb's light chains. M and D are abbreviations for A $\beta$  monomers and dimers, respectively. doi:10.1371/journal.pone.0050317.g006

control antibodies, such as anti-A $\beta$  depleted IVIg, nor was the antibody's reactivity established against A $\beta$  monomers and aggregates. To address these anomalies, we investigated anti-A $\beta$  and control NAbs dose-dependent binding to plate-immobilized A $\beta$  monomers, fibrils, and overlapping A $\beta$  fragments. Our investigations clearly showed that although anti-A $\beta$  NAbs bound to plate-immobilized A $\beta$  monomers and peptide fragments, this reactivity was very weak, in the  $\mu$ M range, and non-specific since similar binding was obtained with the control Nabs. Furthermore, the anti-A $\beta$  NAbs bound  $\sim$ 40-fold more avidly to plate-immobilized A $\beta$  fibrils than the control antibody, confirming that strong Nab-A $\beta$  interactions were critically dependent on the peptide's conformational state.

Natural human antibodies make up about a third of an individual's antibody repertoire, target a wide spectrum of self and non-self antigens, and have been implicated in disease and a plethora of physiological functions [51]. Although the function and molecular basis for anti-A $\beta$  NAbs is not yet known, we have demonstrated their specificity for conformational epitope(s) on A $\beta$  aggregates, dimers to fibrils, and LC fibrils. We have also previously demonstrated that anti-A $\beta$  NAb's are inherently present in normal, presumably healthy individuals, are pan-amyloid fibril reactive, cross-react with CAPS, and have therapeutic potential [11,17,52]. The NAb's ability to cross-

react with a plethora of amyloidogenic assemblies suggests that these IgGs may have evolved to neutralize and/or clear endogenous misfolded proteins containing amyloid-like epitopes in the chaperone-free intercellular milieu. Such conformational binding surfaces presumably contain unique clusters of hydrogen bond donor/acceptor groups, solvent exposed amino acid side chains, and/or a unique chain reversal that are not exposed on natively folded polypeptides [23]. Our ability to isolate anti-A $\beta$  NAbs from IVIg in high salt buffer using Cibacron blue affinity chromatography indicates that these molecules bind a common, limited set of epitope(s) that have a hydrophobic component. However, the molecular composition of these epitope(s) remains elusive since we were unable to isolate anti-A $\beta$  NAbs using a standard hydrophobic matrix, phenyl sepharose CL-4B (Sigma).

In summary, we have demonstrated that anti-A $\beta$  NAbs primarily target conformational epitope(s) on soluble synthetic A $\beta$  assemblies, dimers to fibrils, AD brain-derived A $\beta$ , and these surfaces are similarly exposed on LC fibrils. The latter findings indicate that further investigations on the molecular basis and therapeutic/diagnostic potential of anti-A $\beta$  NAbs are warranted. Although IVIg is limited in supply and there may not be enough to treat the AD patient population, advancing understanding on the molecular basis for NAb-A $\beta$  interactions should facilitate the

generation of a more renewable therapeutic reagent, such as human monoclonal anti-A $\beta$  NAbs.

## Supporting Information

**Figure S1 Quiescent aggregation of [S26CA $\beta$ ]<sub>2</sub>.** (A) Progress curves for the formation of ThT positive material from 22  $\mu$ M [S26CA $\beta$ ]<sub>2</sub> (•) and S26CA $\beta$  monomers (○). The reaction was carried out at 37°C in 40 mM sodium phosphate, pH 7.4. Negative contrast EM was performed on freshly SEC-isolated [S26CA $\beta$ ]<sub>2</sub> (B), and on the aggregation reaction product (C). (D) A high magnification of the image shown in panel C. Scale bar, 100 nm. (TIF)

**Figure S2 Biophysical properties and ThT fluorescence of CAPS and LC fibrils.** Negative contrast EM was performed on 0.2 mg/ml CAPS reaction product (A–B), and on the aggregation products of A $\beta$  (C) and LC (D) fibrils formation reactions. (E) Relative ThT fluorescent signal for 3  $\mu$ g A $\beta$  fibrils, LC fibrils CAPS. (F) Emission wavelength spectra of 50  $\mu$ M CAPS (•), and 50  $\mu$ M of A $\beta$  monomers (○) in PBS, pH 7.4, with excitation at 320 nm. (TIF)

**Figure S3 ThT fluorescence and circular dichroism spectra for A $\beta$  conformers.** (A) Relative ThT fluorescent signal for the same weight (3  $\mu$ g) of WT and S26C A $\beta$  conformers. (B) Circular dichroism spectra obtained for freshly prepared 20  $\mu$ M [S26CA $\beta$ ]<sub>2</sub> (– –), CAPS (–), and WT A $\beta$  monomers (– –) in 25 mM ammonium acetate, pH 8.5. (TIF)

**Figure S4 Acid-induced enhancement of IVIg binding to plate-immobilized A $\beta$ .** (A) Antibody binding curves against plate-immobilized A $\beta$  monomers for IVIg that was unmodified (○), pretreated with acid (0.1 M glycine, pH 3.5), concentrated (Pierce concentrator, 20 kDa m.w.c.o.), and then neutralized with 1 M Tris (pH 9.0) ( $\Delta$ ), or concentrated without treatment with acid/neutralization buffer (•). (TIF)

## References

- Thies W, Bleiler L (2011) 2011 Alzheimer's disease facts and figures. *Alzheimers Dement* 7: 208–244.
- Goedert M, Spillantini MG (2006) A century of Alzheimer's disease. *Science* 314: 777–781.
- Wilcox KC, Lacor PN, Pitt J, Klein WL (2011) Abeta oligomer-induced synapse degeneration in Alzheimer's disease. *Cell Mol Neurobiol* 31: 939–948.
- Benilova I, Karran E, De Strooper B (2012) The toxic Abeta oligomer and Alzheimer's disease: an emperor in need of clothes. *Nat Neurosci* 15: 349–357.
- Lemere CA, Masliah E (2010) Can Alzheimer disease be prevented by amyloid-beta immunotherapy? *Nat Rev Neurol* 6: 108–119.
- Morgan D (2011) Immunotherapy for Alzheimer's disease. *J Intern Med* 269: 54–63.
- Sloane PD, Zimmerman S, Suchindran C, Reed P, Wang L, et al. (2002) The public health impact of Alzheimer's disease, 2000–2050: potential implication of treatment advances. *Annu Rev Public Health* 23: 213–231.
- Britschgi M, Olin CE, Johns HT, Takeda-Uchimura Y, LeMieux MC, et al. (2009) Neuroprotective natural antibodies to assemblies of amyloidogenic peptides decrease with normal aging and advancing Alzheimer's disease. *Proc Natl Acad Sci U S A*. 106: 12145–12150.
- Du Y, Dodel R, Hampel H, Buerger K, Lin S, et al. (2001) Reduced levels of amyloid beta-peptide antibody in Alzheimer disease. *Neurology* 57: 801–805.
- Dodel R, Hampel H, Depboylu C, Lin S, Gao F, et al. (2002) Human antibodies against amyloid beta peptide: a potential treatment for Alzheimer's disease. *Ann Neurol* 52: 253–256.
- O'Nuallain B, Accro L, Williams AD, Koeppen HP, Weber A, et al. (2008) Human plasma contains cross-reactive Abeta conformer-specific IgG antibodies. *Biochemistry* 47: 12254–12256.
- Dodel R, Neff F, Noelker C, Pul R, Du Y, et al. (2010) Intravenous immunoglobulins as a treatment for Alzheimer's disease: rationale and current evidence. *Drugs* 70: 513–528.
- Relkin NR, Szabo P, Adamiak B, Burgut T, Monthe C, et al. (2009) 18-Month study of intravenous immunoglobulin for treatment of mild Alzheimer disease. *Neurobiol Aging* 30: 1728–1736.
- Puli L, Pomeschik Y, Olas K, Malm T, Koistinaho J, et al. (2012) Effects of human intravenous immunoglobulin on amyloid pathology and neuroinflammation in a mouse model of Alzheimer's disease. *J Neuroinflammation* 9: 105.
- Negi VS, Elluru S, Siberil S, Graff-Dubois S, Mouthon L, et al. (2007) Intravenous immunoglobulin: an update on the clinical use and mechanisms of action. *J Clin Immunol* 27: 233–245.
- Magga J, Puli L, Pihlaja R, Kanninen K, Neulamaa S, et al. (2010) Human intravenous immunoglobulin provides protection against Abeta toxicity by multiple mechanisms in a mouse model of Alzheimer's disease. *J Neuroinflammation* 7: 90.
- O'Nuallain B, Hrcic R, Wall JS, Weiss DT, Solomon A (2006) Diagnostic and therapeutic potential of amyloid-reactive IgG antibodies contained in human sera. *J Immunol* 176: 7071–7078.
- Dodel R, Balakrishnan K, Keyvani K, Deuster O, Neff F, et al. (2011) Naturally occurring autoantibodies against beta-amyloid: investigating their role in transgenic animal and in vitro models of Alzheimer's disease. *J Neurosci* 31: 5847–5854.
- Szabo P, Relkin N, Weksler ME (2008) Natural human antibodies to amyloid beta peptide. *Autoimmun Rev* 7: 415–420.
- Solomon B (2007) Intravenous immunoglobulin and Alzheimer's disease immunotherapy. *Curr Opin Mol Ther* 9: 79–85.

**Figure S5 The effect of IVIg on A $\beta$ 's neurotoxicity.** Rat pheochromocytoma PC12 cells (CRL-1721, ATCC) were incubated with 10  $\mu$ M A $\beta$ 1–42 (American Peptide) alone or with 20 mg/ml IVIg. The A $\beta$ 1–42 peptide used was solubilized to ~1 mg/ml in 10  $\mu$ M Tris/HCl (pH 8.6), sonicated in a water bath for 5 min, and 0.1% HCl added to adjusted the pH to 7.2. PC12 cells ( $1 \times 10^5$  cells/ml) were cultured in Neurobasal-A medium with 2% B27 serum substitute and 2 mM L-Glutamine (all from Life Technologies) at 37°C and 5% CO<sub>2</sub>. The cells were seeded into 96-well microplates at 100  $\mu$ l/well and supplemented with 10  $\mu$ l/well of a 20% human serum albumin solution (Baxter). IVIg (Gammagard Liquid, Baxter) dialyzed in Neurobasal-A medium or Neurobasal-A medium alone was added before the cells were incubated with 10  $\mu$ M A $\beta$ 42 in a final volume of 200  $\mu$ l/well. After a 22 h incubation, 2  $\mu$ l/well Triton X-100 was added to determine the maximum LDH release and the plate was incubated for additional 2 h. LDH release from the PC12 cells was determined using the LDH Cytotoxicity Detection Kit (Roche) according the manufacturer's instructions. PC12 toxicity is depicted as optical density (OD). Data represent 6 independent experiments, each performed using 4–8 replicates, and are given as means  $\pm$  SEM. Significant differences between the groups were assessed by one-way ANOVA followed by Tuckey's post hoc test. \*\*\* and \*\* represent p-values of <0.001 and <0.01, respectively, and n.s. indicate not significant. (TIF)

## Acknowledgments

We thank Daniel Kestler, Charles Murphy, and Barry Boland for helpful discussions.

## Author Contributions

Conceived and designed the experiments: BO AS ATW DMW. Performed the experiments: BO ATW ADW HPM LA VB AM SB CH. Analyzed the data: BO ATW ADW HPM LA VB AM DMW SB CH. Contributed reagents/materials/analysis tools: AW MAF HJE HPS DMW. Wrote the paper: BO.

21. Du Y, Wei X, Dodel R, Sommer N, Hampel H, et al. (2003) Human anti-beta-amyloid antibodies block beta-amyloid fibril formation and prevent beta-amyloid-induced neurotoxicity. *Brain* 126: 1935–1939.
22. Szabo P, Mujalli DM, Rotondi ML, Sharma R, Weber A, et al. (2010) Measurement of anti-beta amyloid antibodies in human blood. *J Neuroimmunol* 227: 167–174.
23. O’Nuallain B, Wetzel R (2002) Conformational Abs recognizing a generic amyloid fibril epitope. *Proc Natl Acad Sci U S A* 99: 1485–1490.
24. Town T, Tan J, Sansone N, Obregon D, Klein T, et al. (2001) Characterization of murine immunoglobulin G antibodies against human amyloid-beta1–42. *Neurosci Lett* 307: 101–104.
25. Shankar GM, Walsh DM (2009) Alzheimer’s disease: synaptic dysfunction and Abeta. *Mol Neurodegener* 4: 48.
26. Walsh DM, Selkoe DJ (2007) A beta oligomers - a decade of discovery. *J Neurochem* 101: 1172–1184.
27. Villemagne VL, Perez KA, Pike KE, Kok WM, Rowe CC, et al. (2010) Blood-borne amyloid-beta dimer correlates with clinical markers of Alzheimer’s disease. *J Neurosci* 30: 6315–6322.
28. Mc Donald JM, Savva GM, Brayne C, Welzel AT, Forster G, et al. (2010) The presence of sodium dodecyl sulphate-stable Abeta dimers is strongly associated with Alzheimer-type dementia. *Brain* 133: 1328–1341.
29. Wall J, Schell M, Murphy C, Hrcic R, Stevens FJ, et al. (1999) Thermodynamic instability of human lambda 6 light chains: correlation with fibrillogenicity. *Biochemistry* 38: 14101–14108.
30. O’Nuallain B, Freir DB, Nicoll AJ, Risse E, Ferguson N, et al. (2010) Amyloid beta-protein dimers rapidly form stable synaptotoxic protofibrils. *J Neurosci* 30: 14411–14419.
31. Shevchenko A, Wilm M, Vorm O, Mann M (1996) Mass spectrometric sequencing of proteins silver-stained polyacrylamide gels. *Anal Chem* 68: 850–858.
32. Levine H, 3rd. (1999) Quantification of beta-sheet amyloid fibril structures with thioflavin T methods. *Methods Enzymol*: 274–284.
33. O’Nuallain B, Klyubin I, Mc Donald JM, Foster JS, Welzel A, et al. (2011) A monoclonal antibody against synthetic Abeta dimer assemblies neutralizes brain-derived synaptic plasticity-disrupting Abeta. *J Neurochem* 119: 189–201.
34. Shankar GM, Welzel AT, McDonald JM, Selkoe DJ, Walsh DM (2011) Isolation of low-n amyloid beta-protein oligomers from cultured cells, CSF, and brain. *Methods Mol Biol* 670: 33–44.
35. Betts V, Leissring MA, Dolios G, Wang R, Selkoe DJ, et al. (2008) Aggregation and catabolism of disease-associated intra-Abeta mutations: reduced proteolysis of AbetaA21G by neprilysin. *Neurobiol Dis* 31: 442–450.
36. Li Q, Gordon M, Cao C, Ugen KE, Morgan D (2007) Improvement of a low pH antigen-antibody dissociation procedure for ELISA measurement of circulating anti-Abeta antibodies. *BMC Neurosci* 8: 22.
37. Bohrmann B, Tjernberg L, Kuner P, Poli S, Levet-Trafit B, et al. (1999) Endogenous proteins controlling amyloid beta-peptide polymerization. Possible implications for beta-amyloid formation in the central nervous system and in peripheral tissues. *J Biol Chem* 274: 15990–15995.
38. Shankar GM, Li SM, Mehta TH, Garcia-Munoz A, Shepardson NE, et al. (2008) Amyloid-beta protein dimers isolated directly from Alzheimer’s brains impair synaptic plasticity and memory. *Nat Med* 14: 837–842.
39. Wahlstrom A, Hugonin L, Peralvarez-Marín A, Jarvet J, Graslund A (2008) Secondary structure conversions of Alzheimer’s Abeta(1–40) peptide induced by membrane-mimicking detergents. *FEBS J* 275: 5117–5128.
40. Giacomelli CE, Norde W (2005) Conformational changes of the amyloid beta-peptide (1–40) adsorbed on solid surfaces. *Macromol Biosci* 5: 401–407.
41. Gandy S (2010) Testing the amyloid hypothesis of Alzheimer’s disease in vivo. *Lancet Neurol* 9: 333–335.
42. Golde TE, Das P, Levites Y (2009) Quantitative and mechanistic studies of Abeta immunotherapy. *CNS Neurol Disord Drug Targets* 8: 31–49.
43. DeMattos RB, Bales KR, Cummins DJ, Dodart JC, Paul SM, et al. (2001) Peripheral anti-A beta antibody alters CNS and plasma A beta clearance and decreases brain A beta burden in a mouse model of Alzheimer’s disease. *Proc Natl Acad Sci U S A* 98: 8850–8855.
44. Levites Y, Smithson LA, Price RW, Dakin RS, Yuan B, et al. (2006) Insights into the mechanisms of action of anti-Abeta antibodies in Alzheimer’s disease mouse models. *FASEB J* 20: 2576–2578.
45. Seubert P, Barbour R, Khan K, Motter R, Tang P, et al. (2008) Antibody Capture of Soluble Abeta Does Not Reduce Cortical Abeta Amyloidosis in the PDAPP Mouse. *Neurodegener Dis* 5: 65–71.
46. Weber A, Engelmaier A, Teschner H, Schwarz HP (2009) Gammagard Liquid contains anti-RAGE IGG and SLRP. *Alzheimer Dement*: P146.
47. Deane R, Du Yan S, Subramanian RK, LaRue B, Jovanovic S, et al. (2003) RAGE mediates amyloid-beta peptide transport across the blood-brain barrier and accumulation in brain. *Nat Med* 9: 907–913.
48. Sagare A, Deane R, Bell RD, Johnson B, Hamm K, et al. (2007) Clearance of amyloid-beta by circulating lipoprotein receptors. *Nat Med* 13: 1029–1031.
49. Barlow DJ, Edwards MS, Thornton JM (1986) Continuous and discontinuous protein antigenic determinants. *Nature* 322: 747–748.
50. Klaver AC, Finke JM, Digambaranath J, Balasubramaniam M, Loeffler DA (2010) Antibody concentrations to Abeta1–42 monomer and soluble oligomers in untreated and antibody-antigen-dissociated intravenous immunoglobulin preparations. *Int Immunopharmacol* 10: 115–119.
51. Avrameas S, Ternynck T, Tsonis IA, Lymberi P (2007) Naturally occurring B-cell autoreactivity: a critical overview. *J Autoimmun* 29: 213–218.
52. O’Nuallain B, Williams A, McWilliams Koeppen HP, Acero L, Weber A, et al. (2010) Anti-amyloidogenic activity of IgGs contained in normal plasma. *J Clin Immunol* 30 Suppl 1: S37–42.